# Clay mineral composition of river sediments in the Amazon Basin

**Article** *in* CATENA · October 2007

DOI: 10.1016/j.catena.2007.02.002



**6 authors**, including:

Jean-Loup Guyot
Institute of Research for Development
**846** PUBLICATIONS **14,141** CITATIONS
SEE PROFILE

Leonildes Soares de Melo Filho
Repsol Sinopec Brazil
**26** PUBLICATIONS **285** CITATIONS
SEE PROFILE

Geraldo Boaventura
University of Brasília
**101** PUBLICATIONS **2,291** CITATIONS
SEE PROFILE

C. Lagane
Institute of Research for Development
**76** PUBLICATIONS **1,711** CITATIONS
SEE PROFILE

Available online at www.sciencedirect.com
ScienceDirect
Catena 71 (2007) 340–356
CATENA
www.elsevier.com/locate/catena

# Clay mineral composition of river sediments in the Amazon Basin

J.L. Guyot [a,*], J.M. Jouanneau [b], L. Soares [b,c], G.R. Boaventura [c], N. Maillet [b], C. Lagane [d]

[a] Institut de Recherche pour le Développement (IRD) Laboratoire des Mécanismes de Transfert en Géologie (UMR LMTG), Casilla 18-1209, Lima 18, Peru
[b] Université Bordeaux1, EPOC, CNRS, avenue des facultés 33405 Talence cedex, France
[c] Instituto de Geociências, Universidade de BrasíliaCampus Universitário Darcy Ribeiro, ICC Centro, 70910-900, Brasília, Brazil
[d] Institut de Recherche pour le Développement (IRD) Laboratoire des Mécanismes de Transfert en Géologie (UMR LMTG)38, rue des 36 ponts, F-31400 Toulouse, France

Received 14 July 2006; received in revised form 9 February 2007; accepted 20 February 2007

**Abstract**

Clay minerals are important in evaluating the maturity of suspended sediments, weathering intensity and source area. However, there are processes that can change the mineral assemblage such as river transportation, deposition, remobilization and tributary inputs. In terms of water discharge and sediment yield, the Amazon is one of the largest rivers in the world. Most of the suspended sediments come from the Andes, crossing the lowlands before reaching the ocean. This study measures the spatial distribution of clay mineral assemblages over the entire Amazon basin. The results obtained show the main features of the Amazon River main stem and larger tributaries from their sources to their confluence. Clay mineral composition highlights the evolution of the Madeira and Marañón–Solimões River, which start in the Andes with high illite+chlorite content. Downstream, smectite contents increase. Moreover, all shield tributaries show high kaolinite content. The lower Amazon River is characterized by relative high smectite content, different from the Andean sources. The clay mineral results show that suspended sediments of the Amazon River have three main sources: 1) the Andes mountains; 2) the Amazon shields and 3) the Piedmont basins, especially the Pastaza alluvial megafan and the Fitzcarrald Arch basin. Lateral bank erosion plays also a significant role, by the introduction of more mature sediments into the river, enriched in smectite.


*Keywords:* Clay mineral; River sediments; Amazon basin

## 1. Introduction

Clay minerals may be used as a good indicator of the source area, weathering intensity and maturity of both sedimentary rocks and modern marine and fluvial sediments. As the distance from the source area increases, suspended sediments present a clay mineral assemblage that might have changed in relation to transport (inducing sorting), deposition, bank remobilization (diagenetic processes can occur during temporary storage in the floodplain; illite–kaolinite or smectite for instance) and inputs from different tributaries. Usually illite and chlorite might mark young sediments and soils close to the source areas (mainly plutonic rocks), and smectites characterize badly drained tropical soils. In contrast, kaolinite marks well developed leached soils and mature sediments under tropical climate and more especially high precipitations inducing an intense weathering. However, smectites may also characterize intermediate weathering intensity (Millot, 1964; Gibbs, 1967; Irion, 1984a,b; Johnsson and Meade, 1990; Petschick et al., 1996; Stanley and Wingerath, 1996; Hemming et al., 1998; Saleemi and Zulfiqar, 2000; Thiry, 2000).

Until today, studies in the Amazon basin show that most of the suspended load of the Amazon River (almost 90%) comes from the Andes (Gibbs, 1967; Stallard and Edmond, 1983; Meade et al., 1985; Guyot, 1993; Filizola, 1999, 2003). These sediments present a typical mineralogical signature mirroring

* Corresponding author.
*E-mail addresses:* jean-loup.guyot@ird.fr (J.L. Guyot), jm.jouanneau@epoc.u-bordeaux1.fr (J.M. Jouanneau), leobrasiliensis@yahoo.com.br (L. Soares), grbunb@unb.br (G.R. Boaventura), lagane@lmtg.ups-tlse.fr (C. Lagane).

0341-8162/$ - see front matter © 2007 Elsevier B.V. All rights reserved.
doi:10.1016/j.catena.2007.02.002

the composition of the source area. Results presented up until now were supported by a reduced number of samples, and mainly in the Amazon central floodplain of Brazil.

Gibbs (1967) sampled suspended sediments on a total of 74 points located in the Amazon plain, from areas close to the mountains (Ucayali and Marañón rivers in Peru), to the Amazon River estuary (North Channel in Brazil). The concentration of the Amazon River suspended sediments decreases downstream due to large tributary inputs, changing the Andean signal. Evaluating the mineralogical content, Gibbs distinguished the main tributaries of the Amazon River as coming from a mountain environment (the Andes: Madeira and Solimões rivers) with kaolinite, smectite, chlorite and illite (chlorite+illite contents around 30%), and tropical environment contents (shields: Negro and Tapajós rivers) with high kaolinite and low smectite and chlorite+illite contents.

Irion (1983) described bottom river sediments clay mineral assemblages with 20 sampling points from Pucallpa (Ucayali River, Peru) to the Xingu River confluence in the Amazon floodplain (Brazil). He highlighted the decrease in chlorite content with an increase of smectite and kaolinite downstream.

Johnsson and Meade (1990) described alluvial deposits composition at Macuapanim Island (point bar of the meander and adjacent terrace), on the Solimões River in Brazil. Sediments in these deposits have been exposed to weathering for differing lengths of time since their deposition. In the clay fraction, an increase in the relative abundance of smectite and kaolinite with increasing age, has been observed. Authors conclude that bank erosion and remobilization can be an input of more mature material from the floodplain to the river.

Martinelli et al. (1993) discuss the change of chemical and mineralogical characteristics of river sediments from Vargem Grande near Tabatinga (Solimões River) to Furo do Mugirum near to the estuary, based on 18 bank sediment samples on a 2400 km stretch of the Amazon plain in Brazil. They found that the amount of kaolinite increases as the sediments are transported from their source to the ocean, while smectite and vermiculite decrease and illite remains stable. These observations indicate that sediment maturity increases towards the Atlantic Ocean at the same time as the tropical impact becomes more important.

These previous studies, however, do not cover the whole drainage basin, but only the Solimões–Amazon River main stem in the lowlands. No information exists on tributaries in high mountain areas and intermediate relief areas of the Amazon plain.

This paper aims to show spatial distribution of clay mineral assemblages in river sediments for the entire Amazon basin. The study also attempts to understand the origins and contents, upstream to downstream, of kaolinite, smectite, chlorite and illite in the Amazon River's modern sediments. As a way to characterize the spatial variability along each sub-basin, a large number of samples (229 samples from 146 sites) was collected to include the mountainous basins of the Madeira, Marañón and Napo rivers in Bolivia, Peru and Ecuador, high streams of the shields' sub-basins (Negro, Branco, Trombetas and Jari rivers in the North, Madeira, Tapajós and Xingu rivers tributaries in the South) and the Purus River basin. Samples were also taken along the Amazon River main stem, from the tributary confluences in Peru to Taperinha, as in previous studies.

## 2. The Amazon Basin

The Amazon River basin is the largest hydrographic basin in the world. It covers 6.1 $10^6$ $km^2$ and extends from 48° W (Pará River, Brazil) to 79° W (Chamaya River, Peru), and from 5° N (Cotingo River, Brazil) to 20° S (Parapeti River, Bolivia). This continental basin extends across several countries: Brazil, Peru, Bolivia, Colombia, Ecuador, Venezuela and Guyana (Fig. 1). To the west and southwest, the Andes mountain range borders the Amazon basin, with its highest peaks reaching around 7000 m. However, the Andes represent just 12% of the total surface area (Fig. 2). The Andean rivers (Marañón–Solimões and Madeira tributaries) present profiles with dramatic contrasts, from a steep gradient in the Andean domain to a very low river slope on the Amazon plain: from 20 (Napo River in Peru) to less than 1 cm $km^{-1}$ (Amazonas River in Brazil). The Guyana and Brazil–Central shields represent 44% of the basin. Between the shields and the Andes, there is the Amazonian floodplain domain covering 44% of the entire basin.

The Guiana shield, located in the northern part of the Amazon basin, presents various lithologies: granite complexes, volcanic rocks and sedimentary series (Cordani and Brito Neves, 1982). The Brazil–Central shield, located in the southern and eastern part of the Amazon basin, presents almost the same tectonic evolution as the Guyana shield and some volcano-sedimentary basins (Cordani and Sato, 1999). The Andes mountain range and its associated foreland basin started to develop in the late Cretaceous (Mégard, 1984, Barragán et al., 2005). Tectonic uplift of the eastern Andean Cordillera and modern configuration of the Amazonian foreland basin occurred during Neogene times (Hoorn et al., 1995; Baby et al., 1997, Roddaz et al., 2005). Some parts of the chain show more influence of volcanic deposits as is the case, for instance, in the Ecuadorian Andes. On the other hand, the Bolivian Andes show


Fig. 1. Amazon basin localization.

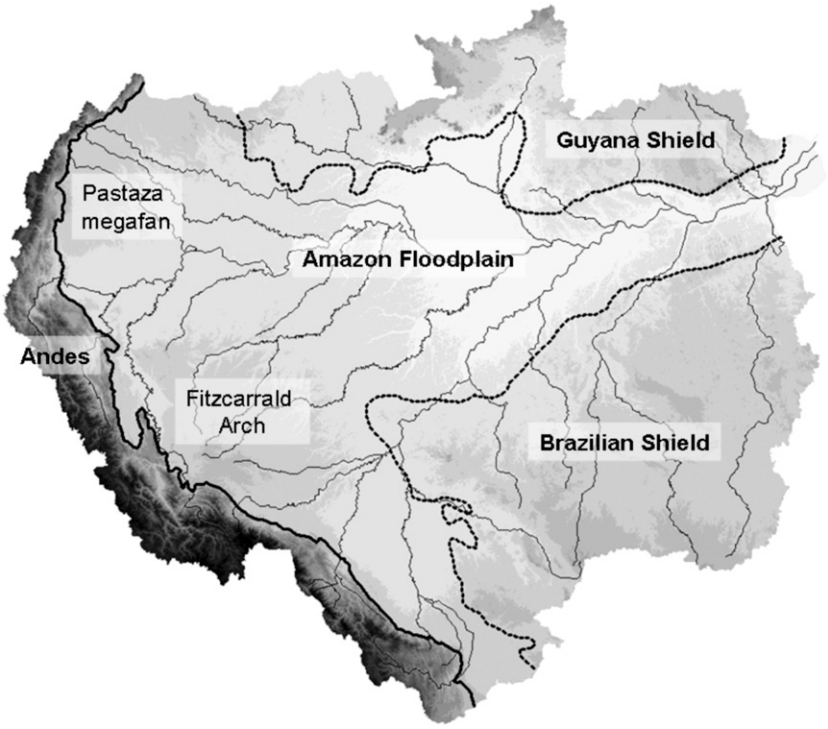


Fig. 2. Amazon basin morphological units, topography from SRTM data.

a strong influence of terrigenous sediments (Audeboud et al., 1973).

The Amazonian floodplain is not a large flat plain, and the western part of this floodplain is deformed by Neogene Andean tectonics: 1. to the North by the presence of a large-scale humid tropical alluvial fan, the Pastaza megafan which could be considered as the largest in the world (Räsänen et al., 1992; Bès de Berc et al., 2005), and to the South by the Fitzcarrald arch relieves (Baby et al., 2005). The modern Pastaza megafan developed in front of the Andean thrust and fold belt and roofs Miocene and Pliocene foreland basin sediments (Curaray formation in Ecuador, Pebas formation in Peru). Currently, its apex is tectonically uplifted by the Subandean wedge thrust system, which induced large scale landslides development and strong fluvial incisions reaching Miocene clayey sediments. The transcontinental Fitzcarrald Arch extends in southern Peru and western Brazil, and constitutes a major geomorphic feature of 420 000 $km^2$, east of the Subandean thrust front. Its relieves, formed by Miocene clayey sediments, reaches an altitude of ~600 m a.s.l., and delimits the Ucayali and Marañon basins from the Madre de Dios basin. The Fitzcarrald Arch uplift is related to the horizontal subduction of the Nazca Ridge below the South American plate, and started probably 5 Ma ago (Espurt et al., in press).

The Amazon Basin receives an average rainfall of 2460 mm $yr^{-1}$, and the average discharge is estimated at 209 000 $m^3$ $s^{-1}$ in the estuary. To the west, the Andean Range constitutes a barrier that blocks the warm and humid air masses coming from the Atlantic Ocean and crossing over the whole basin. In the Andes and their piedmont plains, multiple floods merge downstream to form the great annual flood characteristic of large tropical rivers (Molinier et al., 1996). Due to high precipitation and the steep topographic gradient, the Andean chain is subject to intensive erosion which brings enormous quantities of sediment load to the Andean tributaries of the Amazon River (Guyot, 1993; Masek et al., 1994; Aalto et al., 2006). From the Andean piedmont to the Atlantic Ocean, the sediment transport is characterised by intense sedimentation processes in basins where active subsidence is reported (Baby et al., 1999). It is the case in the Bolivian basin of the Madeira River where only 40% of the eroded load reaches the Amazon River (Guyot et al., 1996), and in the central Amazonian floodplain in Brazil (Dunne et al., 1998; Filizola, 2003; Laraque et al., 2005). On the contrary, from the Andean piedmont to the Amazon River, sediment load on the Napo River increase, representing erosion processes of the Pastaza Megafan (Laraque et al., 2004; Bès de Berc et al., 2005). In Brazil, along the Solimões–Amazon River (2000 km reach), the annual supply of sediment entering the channel from bank erosion is estimated to 1.3 the annual sediment flux of the Amazon River, while the amount transferred from channel to the bars and floodplain represents 1.7 of the same flux (Dunne et al., 1998).

Tropical rainforest covers approximately 5 million $km^2$, which corresponds to 70% of the total Amazon basin area, and the forest covers almost all basin lowlands with some small areas dominated by savannas. Despite the apparent homogeneity of the rainforest, the soil distribution presents certain heterogeneity (Sombroek, 1984; Irion, 1984a). To the east (Eastern and Central Brazil), there are deep soils developed under four Plio-Pleistocene terraces, which are well drained, very acidic, yellow-brown, crumbly, porous, slimy and sandy, showing a predominance of kaolinite in the clay fraction with very low iron oxide content. To the west

(Ecuador, Peru and Western Brazil), the soils (result of weathering of the Solimões formation) are yellow-brown, acidic and often less well drained than in the eastern part of the basin. They are showing an appreciable illite content with kaolinite and oxides (Mn and Fe) in the clay fraction. In addition, podsols are developing over sandy sediments that are the product of the basement shield's erosion. They are usually found in the northern part of the central lowland and may be covered by rain forest or savannas. On the floodplain, the alluvial soils are very badly drained. Their characteristics depend on the sediments provenance and the local periodicity of flooding conditions. In general, the soil clay fraction presents two contrasting types of soil: well-drained soils developing a dominant kaolinite profile; badly drained soils developing a smectite-rich profile (Irion, 1983, 1984a, 1991).

## 3. Methodology

A total of 229 samples were collected by J.L. Guyot on 146 river stations on the whole Amazon basin, from 1986 to 2004 (HYBAM project: www.mpl.ird.fr/hybam). From these 146 river sites; 5 are located outside the Amazon basin: 2 rivers of French Guiana (Maroni and Oyapock rivers) and 3 sites on the Tocantins River basin in Brazil, draining respectively the Guiana and Brazilian shields (Fig. 3).

Samples were collected by hand, below the water table on the river edges, and the sampling point location (latitude and longitude) was determinated with standard GPS (Table 1). The sediment samples were stored in standard hermetic plastic pockets and then dried by atmosphere exposure in the laboratory.

After hydrogen peroxide (30%) treatment to destroy the organic matter, the sediments were re-suspended in a beaker, from which the clay fraction (<2 μm) was extracted after 1h35 using a syringe. The clay mineral study was based on the X-ray diffraction (XRD) analysis of the decarbonated granulometric fraction <2-μm, according to the oriented groundmass technique described by Holtzapffel (1985), using a Phillips monochrome diffractometer with a copper Kα radiation selector.

The identification of minerals was based on their typical reactions to classical treatments: air-dried, ethyl–glycol solvated and heating to 490 °C. Based on glycolated sample diffractograms, semi-quantitative estimates of the different clay minerals were carried out manually by measuring the characteristic reflection areas. The sum of the values obtained for each clay species is determined, and corresponds to 100%. The percentage of each species is then deducted, with a precision of approximately 5%.

## 4. Results

Fig. 3 shows the geographic distribution of sampling points over the Amazon basin, and Table 1 shows the mean total clay mineral assemblage for each point. Altitude data (extracted from SRTM) range from 5 to 3640 m, and show that 75% of sampled points are located below 240 m, and 50% below 130 m high, i.e. mainly along the Amazonian floodplain rivers. In the whole dataset, illite contents vary from 0 to 78% (median 27%), chlorite from 0 to 53% (median 9%), smectite from 0 to 91% (median 15%) and kaolinite from 0 to 100% (median 25%).

### 4.1. Guiana shield tributaries and Negro River basin

As show in Fig. 2, the Guiana shield is drained North by the Maroni (#1) and Oyapock (#2) rivers in French Guiana, and South

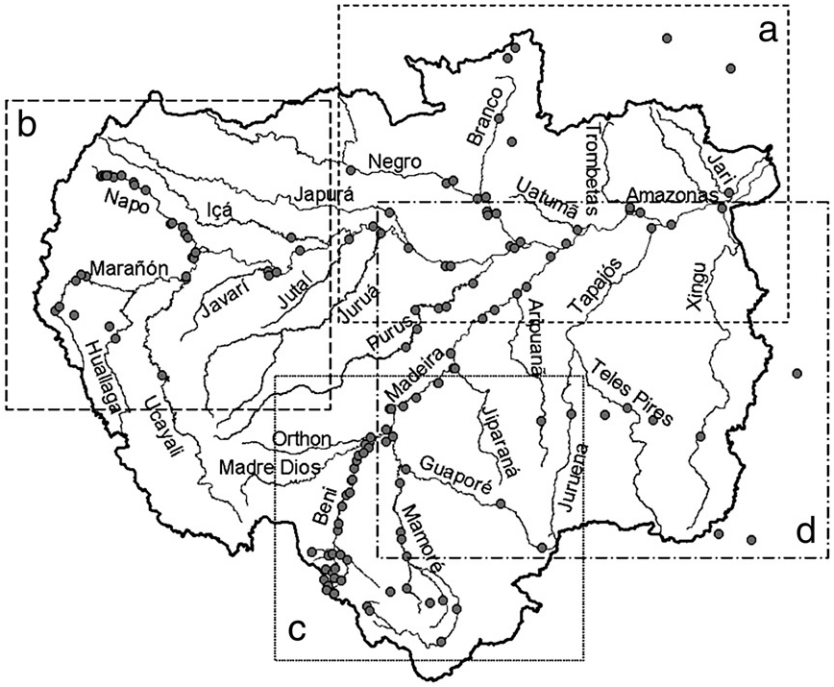


Fig. 3. Sample locations (Boxes a, b, c, d locate detailed maps show in Fig. 4a to d).

Table 1
River sediment clay mineral composition (latitude and longitude in degrees, altitude in meters from SRTM data, clay mineral contents in %)

| Code | Station | River | Latitude | Longitude | Altitude | Samples | Sampling period | Illite | Chlorite | Mixed layers | Smectite | Kaolinite |
|---|---|---|---|---|---|---|---|---|---|---|---|---|
| 1 | Langa Tabiki | Maroni | 4.9862 | −54.4368 | 20 | 1 | 10/02 | 8 | 0 | 0 | 0 | 93 |
| 2 | Saut Maripa | Oyapock | 3.8017 | −51.8847 | 20 | 1 | 10/02 | 0 | 0 | 0 | 0 | 100 |
| 3 | Boca do Jari | Jari | −1.1388 | −51.9902 | 5 | 1 | 06/97 | 14 | 0 | 0 | 30 | 56 |
| 4 | Oriximina | Trombetas | −1.7297 | −55.9025 | 5 | 4 | 03/95–10/96 | 19 | 7 | 3 | 28 | 44 |
| 5 | Oriximina | Nhamunda | −1.7867 | −55.9083 | 5 | 2 | 03/95–07/95 | 22 | 11 | 8 | 43 | 18 |
| 6 | Santana | Uatuma | −2.5692 | −57.9322 | 10 | 1 | 07/95 | 10 | 9 | 6 | 21 | 54 |
| 7 | Bandeira Branca | Cotingo | 4.6400 | −60.4650 | 630 | 1 | 12/96 | 28 | 0 | 0 | 0 | 72 |
| 8 | Vila Surumu | Surumu | 4.1960 | −60.7939 | 130 | 1 | 12/96 | 19 | 0 | 0 | 0 | 81 |
| 9 | Caracarai | Branco | 1.8214 | −61.1236 | 40 | 1 | 12/96 | 16 | 0 | 0 | 0 | 84 |
| 10 | Base Alalau | Alalau | 0.8586 | −60.5200 | 80 | 1 | 12/96 | 0 | 0 | 0 | 0 | 100 |
| 11 | Cachoeira do Caju | Curicuriari | −0.2450 | −67.0180 | 70 | 1 | 07/96 | 0 | 0 | 0 | 0 | 100 |
| 12 | Cfl Negro | Cuiuni | −0.7523 | −63.1117 | 20 | 1 | 03/95 | 0 | 10 | 23 | 0 | 67 |
| 13 | Cfl Negro | Demini | −0.7358 | −62.9243 | 20 | 1 | 03/95 | 2 | 0 | 0 | 0 | 98 |
| 14 | Carvoeiro | Negro | −1.3963 | −61.8770 | 15 | 1 | 03/95 | 4 | 15 | 3 | 4 | 74 |
| 15 | Lago Grande | Jauaperi | −1.3765 | −61.6090 | 15 | 1 | 03/95 | 3 | 0 | 0 | 0 | 97 |
| 16 | Cfl Negro | Jau | −1.9160 | −61.5277 | 15 | 1 | 03/95 | 3 | 14 | 6 | 10 | 68 |
| 17 | Baruri | Carabinari | −2.0153 | −61.5408 | 15 | 1 | 03/95 | 2 | 9 | 11 | 10 | 67 |
| 18 | Posto Funai | Camanau | −1.9310 | −61.2073 | 15 | 1 | 03/95 | 3 | 6 | 4 | 0 | 87 |
| 19 | Paricatuba | Negro | −3.0593 | −60.2518 | 12 | 2 | 03/95–11/95 | 7 | 8 | 2 | 3 | 81 |
| 20 | Site 1 | Napo | −0.4621 | −76.9251 | 250 | 1 | 10/04 | 46 | 17 | 0 | 0 | 37 |
| 21 | Site 2 | Napo | −0.4601 | −76.8711 | 240 | 1 | 10/04 | 30 | 25 | 0 | 0 | 45 |
| 22 | Site 3 | Napo | −0.4332 | −76.7949 | 240 | 1 | 10/04 | 41 | 0 | 0 | 0 | 59 |
| 23 | Site 4 | Napo | −0.4601 | −76.6993 | 230 | 1 | 10/04 | 17 | 0 | 0 | 29 | 54 |
| 24 | Itaya | Napo | −0.4377 | −76.5319 | 230 | 1 | 10/04 | 38 | 20 | 0 | 20 | 22 |
| 25 | Site 6 | Napo | −0.4850 | −76.4281 | 220 | 1 | 10/04 | 35 | 11 | 0 | 37 | 18 |
| 26 | Panacocha | Napo | −0.4782 | −76.3046 | 210 | 1 | 10/04 | 34 | 16 | 0 | 20 | 30 |
| 27 | Tiputini | Napo | −0.7347 | −75.5822 | 180 | 1 | 10/04 | 29 | 14 | 0 | 30 | 27 |
| 28 | Tiputini | Tiputini | −0.8244 | −75.5510 | 180 | 1 | 10/04 | 9 | 0 | 0 | 70 | 22 |
| 29 | Pantoja | Napo | −1.0247 | −75.1216 | 160 | 1 | 10/04 | 30 | 14 | 0 | 31 | 25 |
| 30 | Curaray | Napo | −2.3528 | −74.0789 | 120 | 2 | 12/01–10/04 | 26 | 17 | 0 | 32 | 24 |
| 31 | Curaray | Curaray | −2.3500 | −74.0931 | 120 | 2 | 12/01–10/04 | 13 | 6 | 0 | 60 | 22 |
| 32 | Santa Clotilde | Napo | −2.4818 | −73.6819 | 110 | 1 | 10/04 | 28 | 16 | 0 | 32 | 24 |
| 33 | Cfl. Napo | Tacsha Curaray | −2.7883 | −73.5496 | 100 | 1 | 10/04 | 9 | 0 | 0 | 47 | 45 |
| 34 | Site 21 | Napo | −2.8988 | −73.4872 | 100 | 1 | 10/04 | 19 | 0 | 0 | 53 | 28 |
| 35 | Mazan | Mazan | −3.5100 | −73.1450 | 80 | 1 | 10/04 | 8 | 0 | 0 | 53 | 39 |
| 36 | Puente 24 de Julio | Maranon | −5.7540 | −78.6926 | 430 | 1 | 05/03 | 36 | 14 | 0 | 25 | 25 |
| 37 | Churuja Utcubamba | | −6.0250 | −77.9500 | 1300 | 1 | 05/03 | 46 | 0 | 0 | 28 | 26 |
| 38 | Bagua | Utcubamba | −5.6368 | −78.5567 | 390 | 1 | 05/03 | 16 | 0 | 0 | 64 | 21 |
| 39 | Santa Maria | Nieva | −4.6009 | −77.8670 | 180 | 1 | 05/03 | 20 | 0 | 0 | 52 | 25 |
| 40 | Pinglo | Santiago | −4.4102 | −77.6457 | 160 | 1 | 05/03 | 38 | 18 | 0 | 17 | 27 |
| 41 | Borja | Maranon | −4.4704 | −77.5482 | 150 | 1 | 05/03 | 39 | 14 | 0 | 17 | 30 |
| 42 | Picota | Huallaga | −6.9184 | −76.3248 | 210 | 1 | 05/03 | 31 | 22 | 0 | 26 | 18 |
| 43 | Puente Bolivia | Mayo | −6.4167 | −76.6000 | 270 | 1 | 05/03 | 34 | 18 | 0 | 22 | 26 |
| 44 | Nauta | Maranon | −4.5015 | −73.5602 | 90 | 1 | 12/01 | 26 | 12 | 0 | 38 | 24 |
| 45 | Pucallpa | Ucayali | −8.3800 | −74.5200 | 140 | 1 | 12/01 | 27 | 8 | 0 | 52 | 13 |
| 46 | Cfl Maranon | Ucayali | −4.4794 | −73.4263 | 90 | 1 | 12/01 | 19 | 11 | 0 | 60 | 10 |
| 47 | Iquitos | Amazonas | −3.5988 | −73.1383 | 80 | 1 | 12/01 | 28 | 10 | 0 | 44 | 18 |
| 48 | Iquitos | Nanay | −3.7520 | −73.2859 | 80 | 1 | 12/01 | 3 | 10 | 0 | 20 | 67 |
| 49 | Tabatinga | Solimoes | −4.2545 | −69.9562 | 60 | 1 | 10/95 | 4 | 3 | 0 | 83 | 10 |
| 50 | Cfl Itaquai | Javari | −4.3305 | −70.2095 | 65 | 1 | 10/95 | 12 | 8 | 7 | 62 | 12 |
| 51 | Cfl Javari | Itaquai | −4.3463 | −70.2028 | 65 | 1 | 10/95 | 9 | 7 | 10 | 60 | 15 |
| 52 | Sao Paulo de Olivenc | Solimoes | −3.4503 | −68.9053 | 55 | 1 | 10/95 | 15 | 9 | 7 | 59 | 10 |
| 53 | Ipiranga | Ica | −2.9292 | −69.6948 | 55 | 1 | 10/95 | 10 | 12 | 8 | 61 | 8 |
| 54 | Porto Antunes | Jutai | −2.8793 | −66.9358 | 45 | 1 | 11/95 | 16 | 11 | 5 | 49 | 20 |
| 55 | Fonte Boa | Solimoes | −2.4917 | −66.0748 | 35 | 1 | 11/95 | 16 | 13 | 5 | 54 | 11 |
| 56 | Cfl Solimoes | Jurua | −2.6340 | −65.7935 | 35 | 1 | 11/95 | 8 | 3 | 4 | 79 | 5 |
| 57 | Jacitara | Japura | −1.9060 | −65.2788 | 40 | 1 | 11/95 | 21 | 18 | 7 | 39 | 16 |
| 58 | Tefe | Tefe | −3.4150 | −64.8687 | 30 | 1 | 11/95 | 15 | 10 | 6 | 16 | 54 |
| 59 | Coari | Coari | −4.0608 | −63.1622 | 20 | 1 | 11/95 | 19 | 14 | 5 | 41 | 21 |
| 60 | Itapeua | Solimoes | −4.0517 | −63.0273 | 20 | 1 | 11/95 | 10 | 7 | 3 | 67 | 13 |
| 61 | Labrea | Purus | −7.2197 | −64.7277 | 55 | 1 | 10/96 | 4 | 1 | 0 | 91 | 4 |
| 62 | Canutama | Purus | −6.5555 | −64.3932 | 45 | 1 | 10/96 | 6 | 4 | 0 | 67 | 22 |
| 63 | Cfl Purus | Tapaua | −5.7842 | −64.4078 | 40 | 1 | 10/96 | 6 | 4 | 0 | 67 | 22 |

Table 1 (*continued*)

| Code | Station | River | Latitude | Longitude | Altitude | Samples | Sampling period | Illite | Chlorite | Mixed layers | Smectite | Kaolinite |
|---|---|---|---|---|---|---|---|---|---|---|---|---|
| 64 | Baturite | Purus | −5.7185 | −63.5240 | 35 | 1 | 10/96 | 25 | 8 | 0 | 58 | 9 |
| 65 | Tapaua | Ipixuna | −5.6462 | −63.1965 | 30 | 1 | 10/96 | 19 | 5 | 0 | 39 | 37 |
| 66 | Aruma | Purus | −4.7338 | −62.1555 | 25 | 4 | 03/95–10/96 | 6 | 2 | 2 | 86 | 5 |
| 67 | Manacapuru | Manacapuru | −3.2002 | −60.7678 | 15 | 1 | 11/95 | 9 | 8 | 5 | 52 | 25 |
| 68 | Manacapuru | Solimoes | −3.2985 | −60.6387 | 15 | 2 | 03/95–11/95 | 14 | 9 | 8 | 57 | 13 |
| 69 | Consata | Consata | −15.4000 | −68.5400 | 1040 | 1 | 03/88 | 59 | 34 | 0 | 0 | 7 |
| 70 | Guanay | Mapiri | −15.4913 | −67.8852 | 420 | 3 | 03/88–06/95 | 71 | 20 | 3 | 3 | 2 |
| 71 | Guanay | Tipuani | −15.5028 | −67.8862 | 420 | 3 | 03/88–06/95 | 55 | 16 | 0 | 4 | 25 |
| 72 | Guanay | Challana | −15.5097 | −67.8683 | 420 | 2 | 02/89–06/95 | 50 | 27 | 0 | 3 | 20 |
| 73 | Islani | Zongo | −16.0900 | −68.0400 | 1400 | 1 | 03/88 | 70 | 30 | 0 | 0 | 0 |
| 74 | Yolosa | San Juan | −16.2330 | −67.7396 | 1100 | 1 | 03/88 | 59 | 39 | 2 | 0 | 0 |
| 75 | Santa Barbara | Coroico | −16.1673 | −67.7283 | 810 | 1 | 03/88 | 71 | 29 | 0 | 0 | 0 |
| 76 | Teoponte | Coroico | −15.5015 | −67.8470 | 410 | 3 | 03/88–06/95 | 64 | 30 | 1 | 1 | 4 |
| 77 | Teoponte | Kaka | −15.4912 | −67.8357 | 400 | 2 | 03/88–06/95 | 63 | 22 | 3 | 4 | 10 |
| 78 | Pte Villa | Unduavi | −16.4100 | −67.6600 | 1200 | 2 | 03/88–03/89 | 46 | 53 | 1 | 1 | 0 |
| 79 | Pte Villa | Taquesi | −16.4100 | −67.6500 | 1200 | 1 | 03/89 | 68 | 15 | 0 | 2 | 15 |
| 80 | Achumani | Achumani | −16.5066 | −68.0303 | 3640 | 1 | 03/89 | 78 | 12 | 0 | 4 | 6 |
| 81 | Cfl. Palca | La Paz | −16.7300 | −67.8700 | 2380 | 1 | 03/87 | 60 | 13 | 0 | 14 | 13 |
| 82 | Sapahaqui | Sapahaqui | −16.8800 | −67.9500 | 3130 | 1 | 03/88 | 61 | 30 | 0 | 0 | 9 |
| 83 | Luribay | Luribay | −17.0500 | −67.6600 | 2530 | 1 | 03/88 | 51 | 7 | 0 | 5 | 37 |
| 84 | Plazuela | La Paz | −16.5300 | −67.3700 | 1050 | 1 | 03/89 | 43 | 10 | 0 | 15 | 32 |
| 85 | Cfl Cotacajes | Boopi | −15.6800 | −67.1200 | 450 | 1 | 03/89 | 52 | 28 | 0 | 3 | 17 |
| 86 | Sapecho | Alto Beni | −15.5612 | −67.3713 | 380 | 3 | 03/88–06/95 | 61 | 17 | 1 | 4 | 16 |
| 87 | Angosto Bala | Beni | −14.5273 | −67.4969 | 220 | 20 | 10/87–10/02 | 62 | 19 | 0 | 5 | 13 |
| 88 | Site 1 | Beni | −14.2844 | −67.4737 | 180 | 1 | 10/02 | 62 | 9 | 0 | 6 | 23 |
| 89 | Site 2 | Beni | −13.5713 | −67.3533 | 170 | 1 | 10/02 | 59 | 8 | 0 | 12 | 21 |
| 90 | Site 3 | Beni | −13.1191 | −67.1846 | 160 | 1 | 10/02 | 60 | 8 | 0 | 12 | 20 |
| 91 | Cfl. Beni | Negro | −13.0321 | −67.0363 | 160 | 1 | 10/02 | 58 | 9 | 0 | 8 | 24 |
| 92 | Cfl. Beni | Madidi | −12.5623 | −66.9726 | 150 | 1 | 10/02 | 43 | 9 | 0 | 24 | 25 |
| 93 | Puerto Cavinas | Beni | −12.5121 | −66.9503 | 150 | 1 | 10/02 | 63 | 9 | 0 | 6 | 22 |
| 94 | Fortaleza | Beni | −12.0777 | −66.8819 | 140 | 1 | 10/02 | 55 | 6 | 0 | 18 | 21 |
| 95 | Cfl. Beni | Biata | −11.7500 | −66.7804 | 140 | 1 | 10/02 | 52 | 7 | 0 | 16 | 25 |
| 96 | Pena Amarilla | Beni | −11.5585 | −66.6766 | 140 | 1 | 10/02 | 53 | 7 | 0 | 14 | 25 |
| 97 | Cfl. Beni | Geneshuaya | −11.4249 | −66.4598 | 130 | 1 | 10/02 | 53 | 9 | 0 | 15 | 23 |
| 98 | Portachuelo | Beni | −11.2125 | −66.2488 | 130 | 4 | 10/87–10/02 | 55 | 14 | 0 | 14 | 18 |
| 99 | Miraflores | Madre de Dios | −11.1123 | −66.4159 | 130 | 4 | 10/87–10/02 | 40 | 14 | 0 | 27 | 19 |
| 100 | Caracoles | Orthon | −10.8200 | −66.2000 | 120 | 3 | 10/87–10/02 | 18 | 1 | 2 | 67 | 11 |
| 101 | Cach.Esperanza | Beni | −10.5347 | −65.5812 | 110 | 3 | 10/87–10/02 | 44 | 14 | 3 | 20 | 19 |
| 102 | Puente | Yata | −11.0622 | −65.5105 | 120 | 1 | 06/95 | 49 | 10 | 6 | 18 | 18 |
| 103 | Villa Tunari | Esper. Santos | −16.9700 | −65.4100 | 280 | 2 | 04/88–03/89 | 45 | 41 | 0 | 0 | 15 |
| 104 | Pto Villarroel | Ichilo | −16.8409 | −64.7867 | 200 | 5 | 02/87–03/89 | 50 | 14 | 0 | 2 | 33 |
| 105 | Yapacani | Yapacani | −17.3955 | −63.8436 | 280 | 1 | 03/89 | 37 | 18 | 0 | 19 | 26 |
| 106 | Pte Eisenhover | Pirai | −17.3333 | −63.3167 | 280 | 1 | 03/89 | 48 | 11 | 0 | 4 | 37 |
| 107 | Parotani | Tapacari | −17.5800 | −66.3600 | 2520 | 2 | 04/88–03/89 | 57 | 16 | 0 | 0 | 28 |
| 108 | Capinota | Arque | −17.7300 | −66.2600 | 2380 | 1 | 04/88 | 65 | 14 | 0 | 2 | 19 |
| 109 | Abapo | Grande | −18.9091 | −63.4095 | 440 | 10 | 12/86–05/88 | 63 | 15 | 0 | 5 | 18 |
| 110 | Puerto Pailas | Grande | −17.6546 | −62.7773 | 290 | 2 | 04/88–03/89 | 56 | 14 | 0 | 8 | 23 |
| 111 | Muyurina | Mamore | −15.5800 | −64.7600 | 160 | 1 | 10/87 | 34 | 15 | 0 | 17 | 34 |
| 112 | Pto Almacen | Ibare | −14.8700 | −64.9700 | 150 | 2 | 11/86 | 58 | 12 | 0 | 12 | 20 |
| 113 | Montevideo | Mamore | −14.6100 | −65.0100 | 150 | 2 | 10/87 | 44 | 12 | 0 | 5 | 40 |
| 114 | Cooperativa | Mamore | −12.6600 | −65.0500 | 130 | 2 | 10/87 | 47 | 15 | 0 | 10 | 29 |
| 115 | Pontes e Lacerda | Guaporé | −15.2159 | −59.3536 | 220 | 1 | 06/01 | 23 | 5 | 0 | 29 | 43 |
| 116 | Pimenteiras | Guaporé | −13.4829 | −61.0446 | 160 | 1 | 06/01 | 9 | 0 | 9 | 15 | 67 |
| 117 | Vuelta Grande | Itenez | −12.1200 | −64.8200 | 130 | 2 | 08/87 | 59 | 14 | 0 | 0 | 29 |
| 118 | Guayaramerin | Mamore | −10.8078 | −65.3458 | 110 | 5 | 01/87–10/02 | 46 | 13 | 2 | 14 | 25 |
| 119 | Abuna | Madeira | −9.6733 | −65.4392 | 90 | 1 | 06/95 | 38 | 10 | 3 | 30 | 19 |
| 120 | Abuna | Abuna | −9.6760 | −65.4433 | 90 | 1 | 06/95 | 20 | 5 | 0 | 31 | 44 |
| 121 | Mutum Parana | Mutum Parana | −9.6180 | −64.9333 | 80 | 1 | 06/95 | 3 | 7 | 0 | 0 | 90 |
| 122 | Jacy Parana | Jacy Parana | −9.2580 | −64.3872 | 70 | 1 | 06/95 | 4 | 6 | 0 | 0 | 91 |
| 123 | Cfl Madeira | Candeias | −8.6285 | −63.5547 | 50 | 1 | 06/95 | 21 | 12 | 3 | 4 | 59 |
| 124 | Cfl Madeira | Jamari | −8.6627 | −63.5328 | 50 | 1 | 06/95 | 5 | 0 | 0 | 0 | 95 |
| 125 | Cfl Jiparana | Preto | −8.0738 | −62.8953 | 40 | 1 | 06/95 | 15 | 6 | 0 | 4 | 75 |
| 126 | Calama | Jiparaná | −8.0762 | −62.8868 | 40 | 1 | 06/95 | 9 | 10 | 4 | 6 | 72 |

*(continued on next page)*

Table 1 (*continued*)

| Code | Station | River | Latitude | Longitude | Altitude | Samples | Sampling period | Illite | Chlorite | Mixed layers | Smectite | Kaolinite |
|---|---|---|---|---|---|---|---|---|---|---|---|---|
| 127 | Humaitá | Madeira | −7.4128 | −63.0252 | 35 | 1 | 06/95 | 49 | 10 | 4 | 15 | 22 |
| 128 | Marmelos | Marmelos | −6.2065 | −61.7630 | 30 | 1 | 06/95 | 44 | 11 | 5 | 16 | 24 |
| 129 | Manicoré | Madeira | −5.8165 | −61.3070 | 25 | 1 | 06/95 | 40 | 13 | 2 | 20 | 25 |
| 130 | Aripuanã | Aripuanã | −10.1696 | −59.4661 | 120 | 1 | 06/01 | 11 | 0 | 14 | 11 | 64 |
| 131 | Novo Aripuanã | Aripuanã | −5.1335 | −60.4040 | 20 | 1 | 07/95 | 7 | 0 | 0 | 0 | 93 |
| 132 | Vista Alegre | Madeira | −4.8917 | −60.0283 | 20 | 1 | 07/95 | 32 | 13 | 3 | 36 | 16 |
| 133 | Cfl Amazonas | Madeira | −3.4373 | −58.7938 | 10 | 4 | 07/95–10/96 | 31 | 10 | 3 | 38 | 18 |
| 134 | Itacoatiara | Amazonas | −3.1503 | −58.4660 | 10 | 1 | 11/95 | 18 | 8 | 4 | 34 | 35 |
| 135 | Obidos | Amazonas | −1.9120 | −55.5433 | 5 | 3 | 07/95–10/96 | 16 | 7 | 3 | 58 | 16 |
| 136 | Balsa Ebec–Diauaru | Juruena | −9.8811 | −58.2343 | 200 | 1 | 06/01 | 27 | 0 | 0 | 0 | 73 |
| 137 | Ponte | Apiácas | −9.9357 | −56.9372 | 210 | 1 | 06/01 | 31 | 0 | 0 | 0 | 69 |
| 138 | Ponte | Peixoto de Azevedo | −10.2203 | −54.9669 | 250 | 1 | 06/01 | 21 | 0 | 0 | 0 | 79 |
| 139 | Ponte | Teles Pires | −9.6391 | −56.0191 | 230 | 1 | 06/01 | 18 | 0 | 6 | 6 | 72 |
| 140 | Alter do Chao | Tapajos | −2.4645 | −54.9908 | 5 | 4 | 03/95–10/96 | 7 | 8 | 3 | 4 | 80 |
| 141 | Taperinha | Amazonas | −2.4113 | −54.2615 | 5 | 1 | 10/96 | 22 | 8 | 0 | 50 | 20 |
| 142 | Balsa Sao Felix | Xingu | −10.7774 | −53.1016 | 260 | 1 | 07/01 | 9 | 22 | 0 | 11 | 58 |
| 143 | Porto do Moz | Xingu | −1.7630 | −52.2683 | 5 | 1 | 06/97 | 0 | 0 | 0 | 0 | 100 |
| 144 | Nova Xavantina | das Mortes | −14.6900 | −52.3600 | 260 | 1 | 07/01 | 23 | 0 | 9 | 13 | 55 |
| 145 | Cocalinho | Araguaia | −14.9300 | −51.0700 | 250 | 1 | 07/01 | 13 | 8 | 0 | 25 | 54 |
| 146 | Conceicao do Aragua | Araguaia | −8.2942 | −49.2553 | 160 | 1 | 10/97 | 29 | 0 | 0 | 0 | 71 |

by northern low Amazon River tributaries in Brazil: Jari (#3), Trombetas (#4), Nhamundá (#5) and Uatumã (#6) rivers (Figs. 4a and 5a). A large part of the Negro River basin also lies on the Guiana shield (from #7 to #19). French Guyana rivers and Negro basin tributaries present a clay mineral assemblage dominated by high kaolinite content and minor smectite and illite+chlorite which may represent strongly weathered rocks and soils. The kaolinite content in the Maroni (#1), Oyapock (#2), Curicuriari (#11), Demini (#13), Alalaú (#10) and Jauaperi (#15) rivers reach almost 100%, followed by the Camanaú River (#18) with more than 80% of kaolinite (Fig. 5a). However, the largest left bank tributary, the Branco River, shows almost 80% of kaolinite content with a notable 20% of illite (#7, #8 and #9). For the right bank tributaries of the Negro River: Cuiuni (#12), Jaú (#16) and Carabinani (#17), the clay mineral assemblage is slightly different from that of the left bank tributaries, with kaolinite proportions at around 65%. These tributaries come from the interfluves between the Solimões and Negro rivers, and during the flood period of the Solimões River, some water may overflow into the Negro River tributaries, changing the original shield sign. At Carvoeiro (#14) and Paricatuba (#19), upstream of Manaus City, the Negro River is a balance of these different tributaries, indicating a dominant kaolinite signature, despite the illite+chlorite content. The Jari (#3) and Uatumã (#6) rivers show a relative high kaolinite content (>50%) with minor illite+chlorite, smectite and mixed-layered minerals. For the Trombetas River (#4), kaolinite remains the major clay mineral, but in the Nhamundá River (#5), clay mineral assemblage indicate a mixing with Amazon River waters, due to the existence of some channels (*furos*) which connect this river to the Amazon main stem during the flood periods.

### 4.2. Solimões River basin (Amazon River in Peru)

The Solimões River basin source comes from the Colombian, Peruvian and Ecuadorian Andes, and is named Amazonas River in Peru (Fig. 4b). The Napo River, the main North tributary of the Peruvian Amazon River was intensely sampled during a special field trip (October 2004). Results (Table 1 and Fig. 5b) show an upstream (from #20 to #30) to downstream (#34) evolution from mainly illite+chlorite contents (63%) to mainly smectite content (53%). Right side tributaries of the Napo River: Tiputini (#28), Curaray (#31), Tacsha Curaray (#33) and Mazán (#35) rivers, draining the Pastaza alluvial megafan are characterized by very high smectite contents, up to 70%.

Andean tributaries of the Marañón River in Peru (from #36 to #43, Figs. 4b and 5b) present relative high illite+chlorite contents (around 50%), except for the Utcubamba (#38) and Nieva (#39) rivers, draining large limestones areas, where smectite is largely dominant. At the Andean piedmont (Borja, #41), the Marañón River presents a dominant illite+chlorite clay assemblage (53%), as observed on the Napo River (#20), but with a significant smectite content (17%).

In the Peruvian floodplain, at the Ucayali River confluence, Marañón River at Nauta (#44) presents an intermediate clay assemblage, with illite+chlorite equal to smectite. The Ucayali River in the floodplain (#45, #46) presents a smectite dominant clay assemblage (up to 60%). At Iquitos, the Nanay River (#48) presents high kaolinite contents (67%), when the Amazonas River (#47) shows an intermediate clay assemblage between the Marañón (#44) and Ucayali (#46) rivers.

Downstream in Brazil, Solimões (#52, #55, #60), Içá (#53) and Japurá (#57) rivers, originated in the Andes (Figs. 4a, b, d and 5e), presents the same mixed clay assemblage, with relative high smectite contents. The Solimões River southern tributaries in Brazil, draining the Fitzcarrald arch (Pebas formation in Peru, Solimões formation in Brazil), like Javarí (#50), Itaquaí (#51), Jutaí (#54), Juruá (#56) and Purus (from #61 to #66) rivers

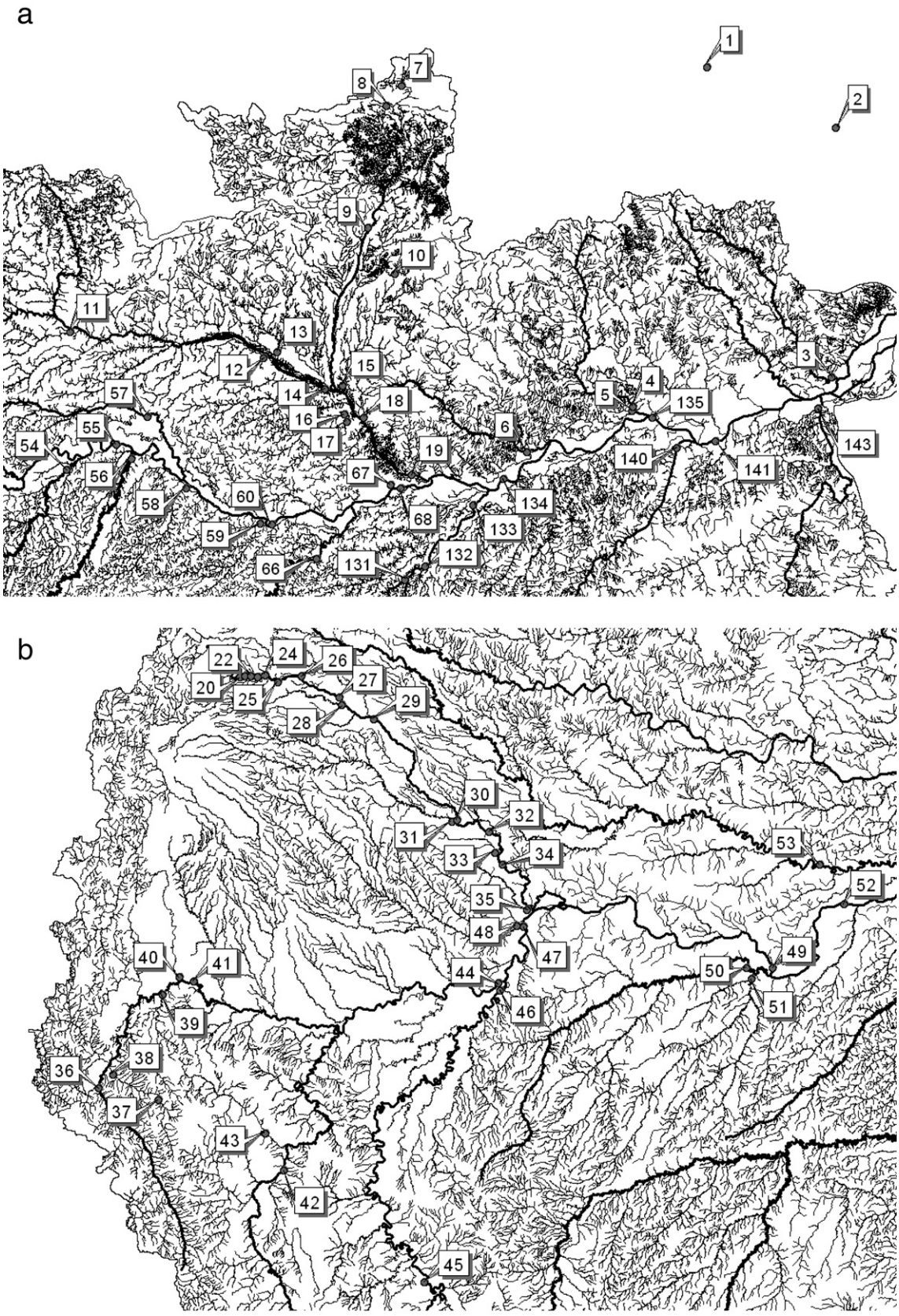


Fig. 4. a — North-East area sampling map, Negro and Amazon River basins (Brazil). (See Table 1 for station number legend). b — West area sampling map, Napo, Marañón and Ucayali river basins (Ecuador and Peru). (See Table 1 for station number legend). c — South area sampling map, Beni and Mamoré river basins (Bolivia and Brazil). (See Table 1 for station number legend). d — Central and South-East area sampling map, Purus, Madeira, Tapajós and Xingu river basins (Brazil). (See Table 1 for station number legend).

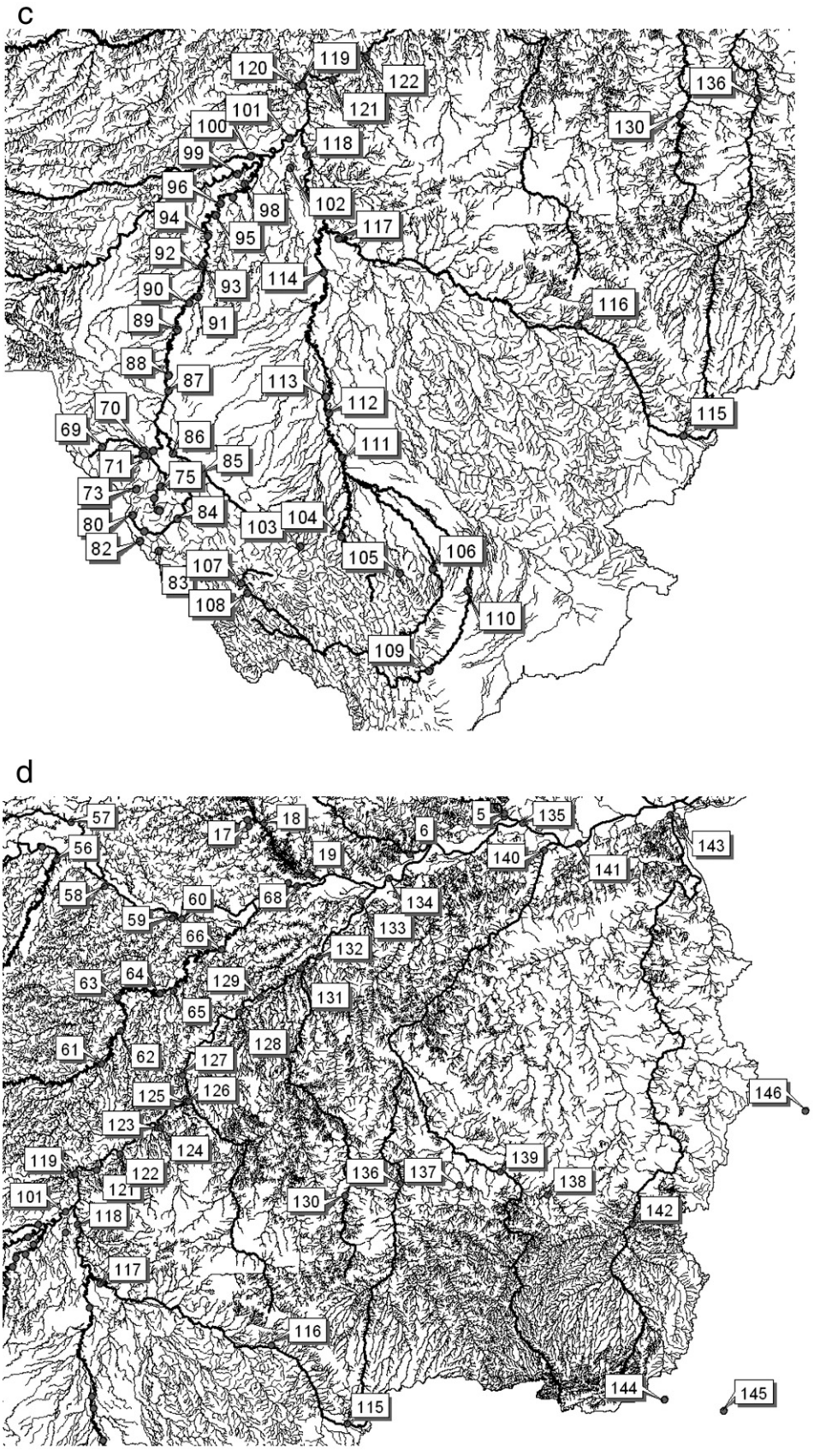


Fig. 4 (*continued*).

present large smectite dominant contents, up to 90% in some stations as Lábrea (#61) and Arumã (#66). The Ipixuna River (#65), right side Purus River tributary, shows major kaolinite content (37%), probably due to the proximity with the Brazilian shield. At the confluence with Negro River, the Solimões River at Manacapuru (#68) shows a smectite dominant (57%) clay assemblage.

### 4.3. Madeira River basin

In the Andean tributaries of the Madeira River basin in Bolivia (Table 1, Fig. 4c), the dominant sediment clay minerals are illite and chlorite (Fig. 5c and d). In the Andean Beni River basin (from #69 to #87), illite+chlorite represent more than 90% in all sampled river sites above 1000 m high, except in the

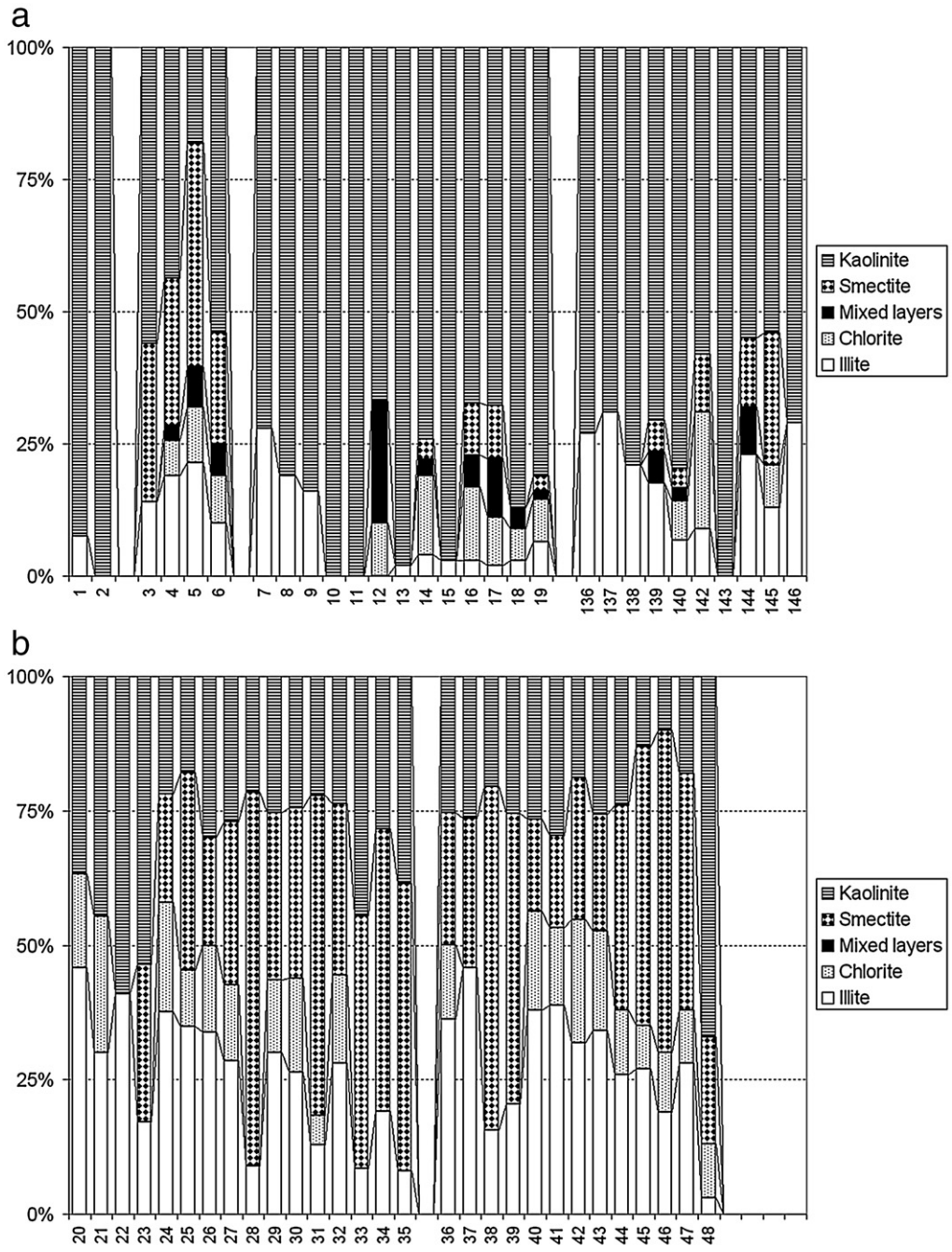


Fig. 5. a — Clay mineral composition of French Guiana rivers (#1 and #2), Northern tributaries of the Amazon river in Brazil (#3 to #6), Negro basin rivers (#7 to #19), Tapajós basin rivers (#136 to #140), Xingu basin rivers (#142 and #143), and Tocantins basin rivers (#144 to #146). (See Table 1 for station number legend). b — Clay mineral composition of Napo basin rivers (#20 to #35), Marañón basin rivers (#36 to #45), Ucayali basin rivers (#45 and #46), and Amazonas basin rivers in Peru (#47 and #48). (See Table 1 for station number legend). c — Clay mineral composition of Beni basin rivers in Bolivia (#69 to #101). (See Table 1 for station number legend). d — Clay mineral composition of Mamoré basin rivers in Bolivia (#102 to #118), Madeira basin rivers in Brazil (#119 to #133). (See Table 1 for station number legend). e — Clay mineral composition of Solimões and Purus basin rivers (#49 to #68), and Amazon basin rivers in Brazil (#134, #135 and #141). (See Table 1 for station number legend).

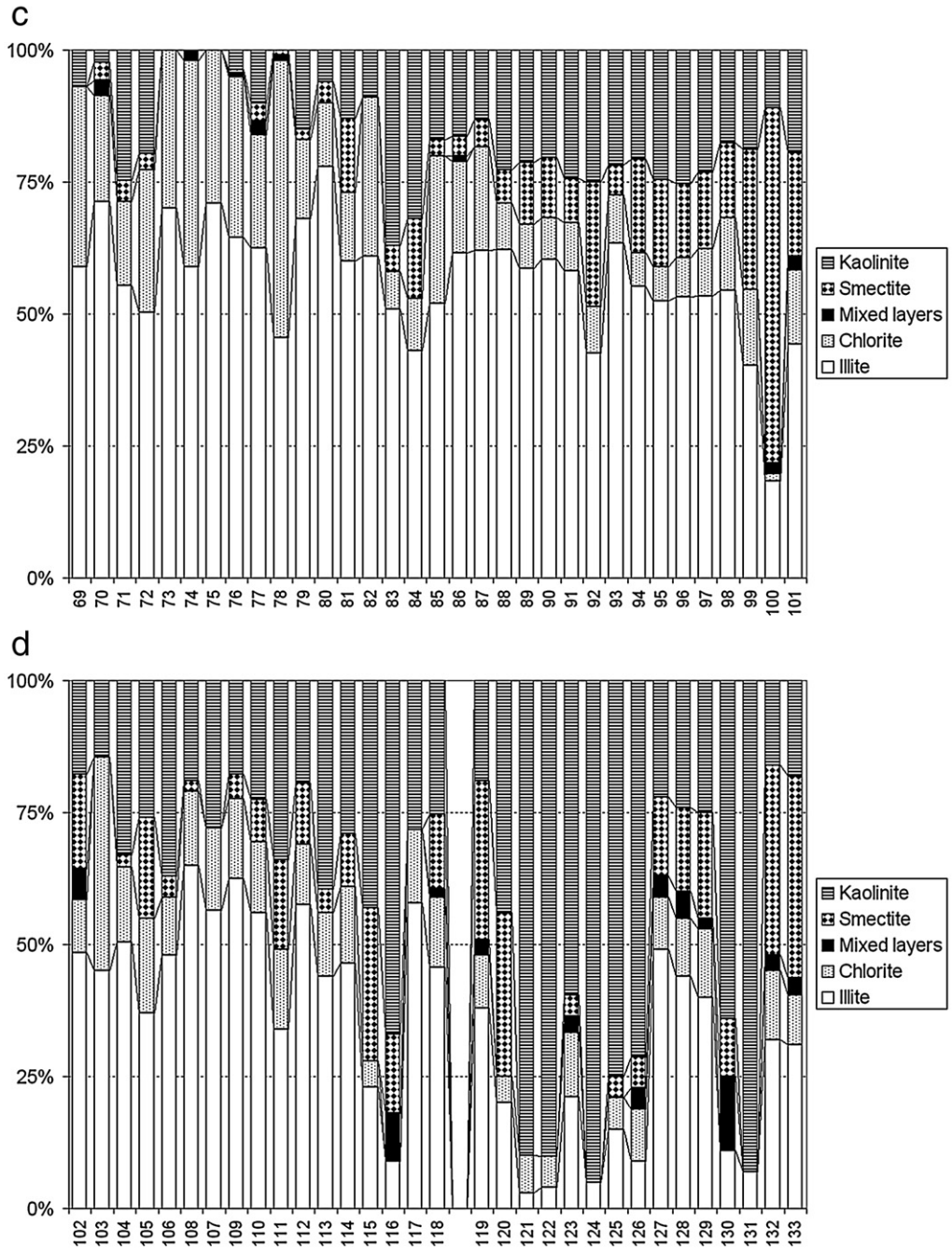


Fig. 5 (*continued*).

La Paz River basin (#81, #83, #84) where significant kaolinite or/and smectite can be observed. Downstream, in the Sub-andean Guanay area (#71 and #72), relative high kaolinite contents are also noted. At the Andean piedmont, the Beni River at Angosto del Bala (#87) presents a clay mineral assemblage with a high illite+chlorite signature (81%). For the Andean rivers of the Mamoré River basin (from #103 to #109), illite+chlorite is also the dominant assemblage, with kaolinite as second importance. At the Andean piedmont, the Grande River at Abapo (#109) presents a much more similar clay assemblage than that observed on the Beni River (#87).

In the Bolivian floodplain (Table 1, Fig. 5c and d), the Beni River was sampled intensively during a special field trip realized in October 2002 (Fig. 4c). Results obtained along the Beni River from the Andean piedmont (#87) to Portachuelo (#98), near the Madre de Dios River confluence, show a light decrease of illite+chlorite, and increase of kaolinite and/or smectite. Just before the confluence with the Mamoré River, at Cachuela Esperanza (#101), the Beni River shows intermediate clay mineral composition between the Madre de Dios (#99) and Beni (#98) rivers. Such behaviour is expected because the Madre de Dios River represents 50% of the total discharge. The Orthon River

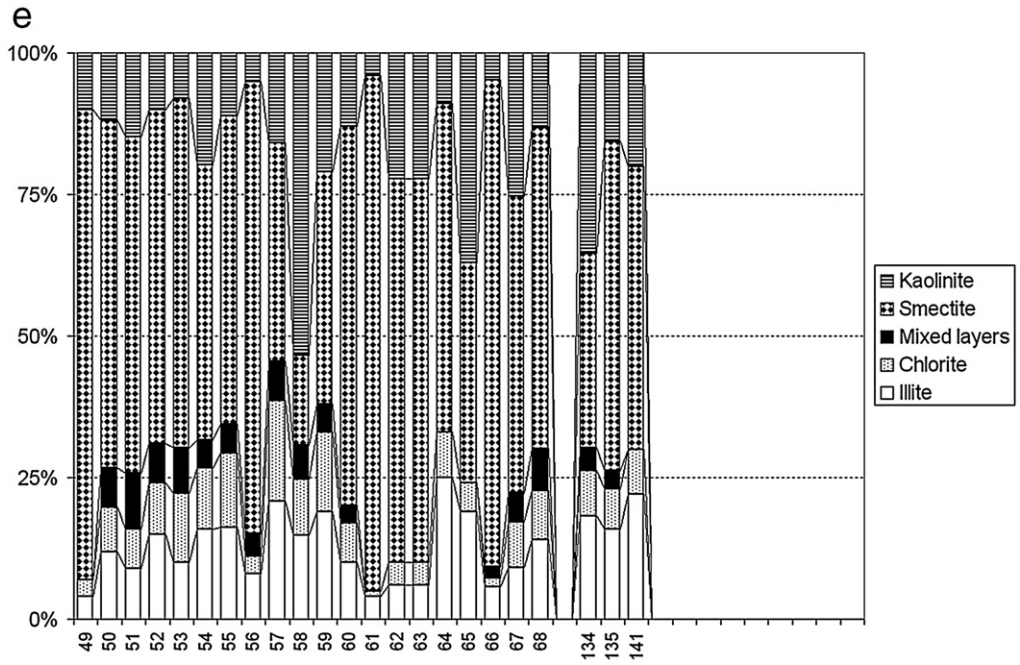


Fig. 5 (*continued*).

(#100), which comes from the Tertiary series of the Fitzcarrald Arch (Acre Formation) like the Purus, Juruá and Javari rivers in Brazil, presents very high smectite content (67%).

The Mamoré River (#111, #113, #114, #118) presents in the Bolivian floodplain a high illite+chlorite content, with relative enrichment in kaolinite. The Ibaré floodplain river (#112) clay mineral assemblage is comparable to that of the Mamoré River (an Andean river), resulting mainly from the invasion of the Mamoré River waters during flood periods (Guyot et al., 1991). The Itenez (Guaporé) River, the largest eastern tributary of the Mamoré River, which drains the Brazil–Central shield (66% of its basin), shows upstream a kaolinite dominant clay assemblage (#115, #116), while the downstream station (#117) presents a clay mineral assemblage similar to that of the Mamoré River, probably due to the same phenomenon of invading waters from the Mamoré River during the high water period.

The right-hand tributaries of the Madeira River basin in Brazil, draining the Brazilian shield (Figs. 4d and 5d) show a very high kaolinite content (up to 95%), which indicates a source area composed of strongly weathered rocks and soils (from #121 to #126, #130 and #131). However, the Marmelos River (#128) shows a mineral assemblage that stands out among the other shield tributaries. This can be explained by the proximity of sampling locations near from the confluence, indicating an input of Madeira River suspended sediment. Among all the Madeira River tributaries, the Abunã River (#120) can be highlighted because it is the only left-hand tributary. Moreover, this river shows a clay mineral assemblage with a relative high smectite content, which can be explained by the same reasons as for the Orthon River (#100): both rivers come from the Tertiary sedimentary series (Fitzcarrald Arch). As for the Beni River, there is an evident decrease of the illite+chlorite contents in the Madeira main stem, from Humaitá to the confluence with the Amazon River (#127, #129, #132 and #133), where smectite contents increase.

### 4.4. Other Brazilian shield tributaries

The Brazilian shield is drained by right side tributaries of the Madeira River (see above), but also by the Tapajós (from #136 to #140) and Xingu (#142 and #143) basin rivers, two large southern tributaries of the Amazon River (Figs. 4d and 5a). All the sampled points present a net kaolinite dominant clay assemblage characteristic of this region of the Amazon basin. As for the Guyana shield, 3 river points where sampled outside the Amazon basin, on some Araguaia tributaries (from #144 to #146), the main affluent of the Tocantins River, located east to the Amazon basin.

### 4.5. Amazon River main stem in Brazil

The Amazon River main stem starts in Brazil near Manaus at the Solimões and Negro rivers confluence (Figs. 4a and 5e). The Madeira River then flows into the Amazon River, completing the main hydro geochemical frame. The Amazon River (#134, #135, #141) presents a clay mineral assemblage similar to a mixing of Madeira (#133) and Solimões (#68) rivers, where smectite represents up to 50%, then illite and chlorite (30%) and finally kaolinite (20%).

## 5. Discussion

The results obtained on the whole Amazon basin seem to show that geographical distribution of the clay minerals is controlled by

different sources. The clay mineral assemblages thus make it possible to trace the source of the sediment material.

### 5.1. Guiana and Brazilian Shields rivers

In North, rivers draining the Guiana shield (Table 1, Figs. 4a and 5a) are largely characterized by a clay assemblage with dominant kaolinite, with contents exceeding 70% (#7, #14), 80% (#8, #9, #18, #19), 90% (#1, #13, #15) and reaching 100% on some sites (#2, #10, #11). At the South, rivers from the Brazilian shield (Table 1, Figs. 4d, 5a and d) present a similar clay assemblage, where the contents of kaolinite exceed 70% (#125, #126, #136, #138, #139, #146), 80% (#140), 90% (#121, #122, #124, #131), or reach even 100% (#143). The kaolinite, produced by intense weathering in humid tropical environments, seems to be the characteristic clay mineral of the Guyana and Brazilian shields.

### 5.2. Andean rivers

In the Andean basins, there are some regional differences. In Bolivia, on the high Madeira River basin where sediment erosion rates are particularly high (Guyot, 1993), the Andean tributaries of the Beni River (Table 1, Figs. 4c and 5c) are characterized by a clay assemblage with strong dominant illite+chlorite content, which often exceeds 70% (#71, #72, #81, #86), 80% (#77, #79, #85, #87), 90% (#69, #70, #73, #74, #76, #78, #80, #82) and can reach 100% (#75). In the Andean basin of Mamoré River (Table 1, Figs. 4c and 5d), the results are similar, with contents of illite+chlorite frequently higher than 70% (#107 to #109) and 80% (#103). At the two principal Andean piedmont stations: Angosto del Bala on Beni River (#87) and Abapo on the Grande River (#109), the clay assemblage respectively shows a illite+chlorite content of 81% and 78%. The signature illite+chlorite, representing young sediments, thus seems to be characteristic of the Andean rivers of Bolivia, where the strongest rates of physical erosion of the Andean chain are observed (Guyot et al., 1996, Aalto et al., 2006).

Despite actual cold mountain climatic conditions, some Andean tributaries of the Beni and Mamoré rivers, like La Paz (#84), Luribay (#83), Yapacani (#106) or Pirai (#106), draining Plio-Quaternary sedimentary series, show a higher kaolinite content (from 26% to 37%). The same clay assemblage was found in recent sediments of Bolivian highland lakes (Titicaca and Poopo), coming from similar Plio-Quaternary sedimentary sequences (Boulangé et al., 1981).

The Andean tributaries of Marañón River in Peru (Table 1, Figs. 4b and 5b) present a less contrasted clay assemblage, with illite+chlorite varying from 46% to 56%, and contents of kaolinite and smectite of about 20–30%. However, two right bank Andean tributaries of Marañón River (#38, #39) show relative high content of smectite (>50%). These two rivers drain thick Cretaceous and Jurassic limestone series, basin characteristic which can explain this difference. Lastly, at the Borja station (#41) located at the Andean piedmont, Marañón River shows a mineralogical assemblage with light dominant illite+chlorite (53%), then kaolinite (30%) and smectite (17%). On the Napo River in Ecuador (Table 1, Figs. 4b and 5b) observed near the Andean piedmont (#20) indicate a clay assemblage with illite+chlorite dominating (63%).

North (Ecuador) to South (Bolivia), the Andean clay mineralogical assemblage is illite+chlorite dominant, more strong in the South (Beni and Mamoré river basins) where the Andean chain primarily consists of detritical series, than in the North where thick Andean limestone series crop out (Marañón River basin), as well as active volcanism (Napo River basin). Lastly, inside the Andes, certain rivers can present assemblages relatively rich in kaolinite, because of the presence of Tertiary sedimentary sequence, from Miocene to Plio-Quaternary, as the La Paz area rivers in Bolivia.

### 5.3. Amazon floodplain rivers

In the Amazon floodplain, the clay assemblage is not uniform, but variable from one basin to another. All the Napo River right bank tributaries (Table 1, Figs. 4b and 5b), which drain the Pastaza alluvial megafan (#28, #31, #33, #35) are dominated by smectite (from 47 to 70%), while kaolinite is also well represented (from 22 to 45%). The same mineralogical frame is observed on the Southern tributaries of the Solimões River in Brazil draining the Fitzcarrald arch, like Javari, Itaquaí, Juruá and Purus rivers (Table 1, Fig. 4b and d), and where smectite exceeds 60% (#50, #51, #62, #63), 70% (#56), 80% (#66), and 90% (#61). In the Beni floodplain of Bolivia, the Orthon River (#100), which drains a part of the Fitzcarrald arch close to the Purus River in Brazil, presents the same smectite rich contents (67%). Because of the current tectonic movements, the small relieves of Pastaza megafan and Fitzcarrald arch, consisted of sedimentary series originating from the Andes, are subjected today to erosion (Laraque et al., 2004; Bès de Berc et al., 2005). It appears that the clay product of this erosion presents a characteristic signal with dominant smectite. These smectites come from the Pebas Sea clay deposits, which are eroded on the Fitzcarrald Arch (Baby et al., 2005); and form also the Pastaza megafan substratum (Formation Curaray) where they are also eroded (Roddaz et al., 2005, 2006).

It is not easy to determine the clay mineral assemblage for the other floodplain rivers, first because these rivers present very weak sediment load, and then because there is a substantial mixing by Andean rivers near the confluences. It is particularly the case with the Nhamundá River (#5) contaminated by the Amazon River, the Ibaré (#112), Guaporé (#117) and Marmelos (#128) contaminated by the Mamoré–Madeira River, and the Manacapuru lake (#67) by the Solimões River. In some cases, Amazonian floodplain rivers are dominated by kaolinite, as the Nanay River (#48) in Peru, or Tefe River (#58) in Brazil. In the case of Nanay River, the presence of kaolinite can be explained by the proximity of the Iquitos arch, constituted by shield weathering products (Roddaz et al., 2006).

### 5.4. Andean rivers crossing the Amazon floodplain

When Andean rivers cross the Amazon floodplain, the clay mineral assemblage can change from upstream to downstream,

depending on the lateral river yields and/or bank erosion and remobilization. From the Andean piedmont (#20) to the Amazon confluence (#34), clay mineralogy evolution along the Napo River (620 km) show a progressive increase of smectite and decrease of illite+chlorite due to lateral yields coming from the Pastaza alluvial megafan. The increase in smectites is obvious as one alters the clay sediments of Formation Pebas (Roddaz et al., 2005).

The downstream evolution along the Beni–Madeira River (Table 1, Fig. 6a), from Andean rivers of Bolivia (Coroico and Kaka rivers), to the Madeira River confluence in Brazil (#133), shows a progressive diminution of the illite+chlorite assemblage, with 100% to 85% in the Andes (#75 to #77), 81% at the Andean piedmont (#87), 58% at the Bolivia–Brazil frontier (#101), and finally 41% at the Amazon River confluence (#133). The exit of the Andes is represented by an increase of kaolinite, which remains constant along the floodplain crossing. The floodplain crossing is characterized by a progressive increase of smectite, from 5 to 38%, as suggested by Johnsson and

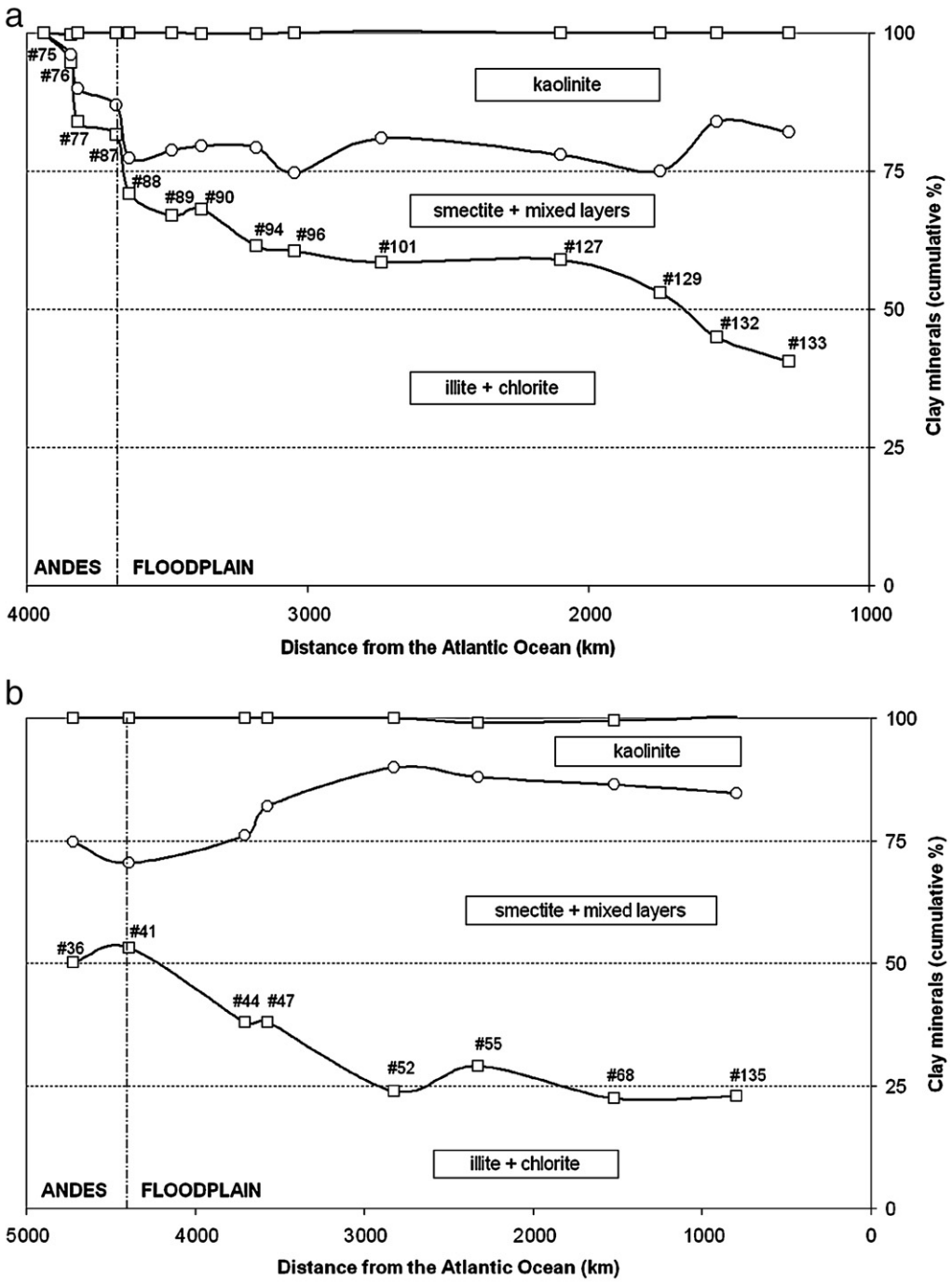


Fig. 6. a — Downstream evolution of clay mineral composition along the Beni – Madeira River. (See Table 1 for station number legend). b — Downstream evolution of clay mineral composition along the Marañón – Solimões – Amazon River. (See Table 1 for station number legend).

Meade (1990). The same trend is observed along the other Bolivian large floodplain river (Grande–Mamoré River), from Abapo (#109) located at the Andean piedmont, to Guayaramerin (#118) at the Beni River confluence, with the illite+chlorite assemblage from 78 to 59%. These data confirm the importance of lateral yields (bank erosion and remobilization) as well as the sedimentary trapping to the foot of the Andes in the tectonic foreland basin (Guyot et al., 1996).

The Marañón–Solimões River presents a downstream evolution (Table 1 and Fig. 6b) with the same tendencies as observed on the Beni–Madeira River, with a progressive decrease of the illite+chlorite content, from the Peruvian Andean piedmont (Borja) to the Amazon River in Brazil (São Paulo de Olivença), with values from 53% (#41) to 24% (#52). This region is also characterized by a kaolinite content decrease and a large increase of smectite content, from 17% (#41) to 59% (#52), probably due to bank erosion sediment remobilization, and sediment yield coming from the Tertiary series (Pastaza Megafan and Fitzcarrald Arch). In the central and lower Brazilian Amazon floodplain, where large sediment exchanges between channel and floodplain are observed (Dunne et al., 1998), there is no evident trend along the Solimões–Amazonas River (Fig. 6b), from São Paulo de Olivença (#52) to Obidos (#135).

These results on the whole Amazon drainage basin permit us to identify three main sources of clay mineralogy: 1. the shield domain with high kaolinite contents, 2. the Andean domain (mainly Palaeozoic silicoclastic series) with the illite+chlorite predominant assemblage, and the Miocene sediment series, like the Pastaza Megafan (Cururay and Pebas formations), Fitzcarrald Arch (Pebas and Solimões formations), which high smectite contents. The ternary diagram (Fig. 7) corroborates the three main sources of Amazon sediments, and shows the floodplain crossing evolution.

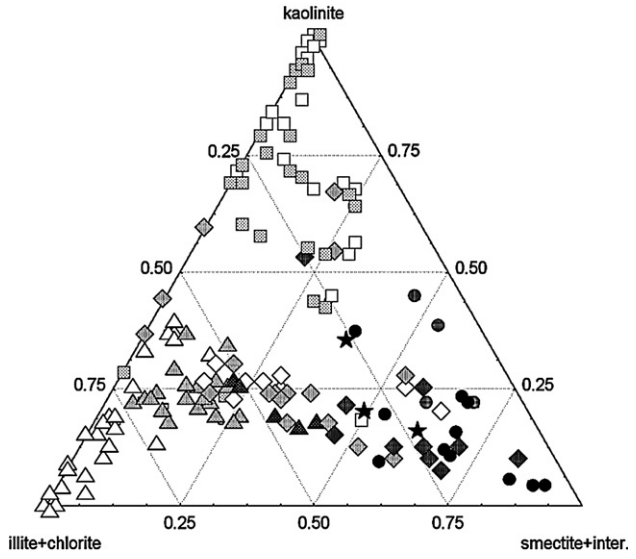


Fig. 7. Relative clay mineral composition of Amazon River basin tributaries, indicating source area □: Guiana Shield, ▨: Brazilian Shield, △: Bolivian Andean tributaries of Madeira river, ◬ Bolivian floodplain tributaries of Madeira river, ▲: Brazilian floodplain tributaries of Madeira river, ◇: Peruvian Andean tributaries of Solimões river, ◈: Peruvian floodplain tributaries of Solimões river, ◆: Brazilian floodplain tributaries of Solimões river, ◍: Pastaza Aluvial Megafan tributaries, ●: Fitzcarrald Arch basin tributaries, ★: Amazon river in Brazil.

The Guyana shield rivers (white squares) and the Brazilian shield rivers (grey squares) plot into the kaolinite pole. Rivers draining the Miocene sedimentary series from the Fitzcarrald Arch (black circles) or the Pastaza megafan (grey circles) plot near the smectite pole. The Madeira River basin (triangles), Andean rivers (white triangles) plot into the illite+chlorite pole, with sometimes notable contents of kaolinite. Crossing the Bolivian Amazonian floodplain, the Beni and Mamoré rivers (grey triangles) increase in smectite content, and this trend is accentuated in Brazil along the Madeira River (dark grey triangles). For the Marañón–Solimões River basin (diamonds), Andean rivers in Peru (white diamonds) plot mainly as Bolivian Andean rivers, and the same enrichment in smectite is observed along the Peru floodplain crossing (grey diamonds) and in Brazil (dark grey diamonds). This smectite enrichment can be an input of more mature material from the floodplain (bank erosion) to the river (Johnsson and Meade, 1990). Finally, the Amazon River (black stars) presents an intermediate clay mineral assemblage, closer to the smectite pole.

According to Gibbs (1967); Meade et al. (1985); Guyot (1993); Filizola (1999, 2003), the largest main source of the Amazonian suspended sediment is the Andes (almost 90%). It might be expected to find high proportions of illite and chlorite downstream. However, the Amazon River presents a progressive upstream — downstream enrichment of smectite, and in Brazil the Amazon River does not present an Andean clay mineral assemblage, as observed in the piedmont rivers. This evolution can be interpreted by lateral bank erosion along the large floodplain crossing as described by Dunne et al. (1998), but also by the input from rivers draining the Tertiary sediment series, like Pastaza Megafan in the North and Fitzcarrald Arch in the South.

Furthermore, the kaolinite contents become slightly weaker, showing that the shield tributaries do not make a strong impact because they present very low sediment loads (Filizola, 1999).

## 6. Conclusion

Clays from all the rivers draining the Guiana and the Brazilian shields present a typical clay assemblage with high kaolinite content, up to 100% in some rivers. In spite of the large spatial extend of these shield basins, the kaolinite content in the Amazon main stem remains low because of the very low sediment load delivered from these basins.

The Andes range presents a typical signature with relative high illite+chlorite contents, than can be observed on the Andean piedmont for all the main tributaries of the Amazon basin: 63% for the Napo River, 53% for the Marañón River, 53% for the Huallaga River, 81% for the Beni River, and 78% for the Grande River.

Crossing into the Amazon floodplain, the Andean rivers show a notable enrichment in smectite, provided by lateral bank erosion as suggested by Johnsson and Meade (1990), and/or from tributaries draining large Miocene sediment series such as the Pastaza megafan to the North or the Fitzcarrald Arch to the South. These results of clay mineral analysis show that the

Amazon basin sediment load increases in maturity as it progresses downstream, as evidenced by Dosseto et al. (2006).

In Brazil, Amazon River sediment presents a clay assemblage (mainly smectite) that is not typically Andean. There, the large sediment yield exported to the Atlantic ocean (Guyot et al., 2005) is not coming directly from the Andes, but is the mixing of Andean fresh sediment, bank remobilization, and recycled sediment from Tertiary series in the basin.

## Acknowledgments

All field sampling was part of the HYBAM Program (www.mpl.ird.fr/hybam), and the clay analysis was shared between the Universities of Brasília (Brazil), Bordeaux and Toulouse (France). Our deepest thanks to our numerous traveling companions, along the Amazonian rivers or on the Andean tracks, without whom this database could not have existed. Lastly, we thank Patrice Baby for his useful comments concerning geology of the Amazon basin. We also thank the CNPq Agency for Brazil for the financial support brought to this study (PhD grant for Leonildes Soares).

## References

Aalto, R., Dunne, T., Guyot, J.L., 2006. Geomorphic controls on Andean denudation rates. Journal of Geology 114 (1), 85–99.

Audeboud, E., Capdevila, R., Dalmayrac, B., Debelmas, J., Laubacher, G., Lefevre, C., Marocco, R., Martinez, C., Mattauer, M., Megard, F., Paredes, J., Tomasi, P., 1973. Les traits géologiques essentiels des Andes centrales (Pérou–Bolivie). Revue de Géographie Physique et de Géologie Dynamique 6, 73–114.

Baby, P., Rochat, P., Mascle, G., Hérail, G., 1997. Neogene shortening contribution to crustal thickening in the back arc the Central Andes. Geology 25, 883–886.

Baby, P., Guyot, J.L., Deniaud, Y., Zubieta, D., Christophoul, F., Rivadeneira, M., Jara, F., 1999. The High Amazonian Basin: tectonic control and mass balance. Proc. Hydrological and Geochemical Process in Large-Scale River Basins, Manaus, Brazil.

Baby, P., Espurt, N., Brusset, S., Hermoza, W., Antoine, P.O., Roddaz, M., Martinod, J., Bolaños, R., 2005. Influence of the Nazca ridge subduction on the Amazonian foreland basin deformation: Preliminary analyses. Proc. 6th International Symposium on Andean Geodynamics (ISAG 2005, Barcelona), Extended Abstracts, pp. 83–85.

Barragán, R., Baby, P., Duncan, R., 2005. Cretaceous alkaline intra-plate magmatism in the Ecuadorian Oriente Basin: geochemical, geochronological and tectonic evidence. Earth and Planetary Science Letters 236, 670–690.

Bès de Berc, S., Soula, J.C., Baby, P., Souris, M., Christophoul, F., Rosero, J., 2005. Geomorphic evidence of active deformation and uplift in a modern continental wedge-top-foredeep transition: example of the eastern Ecuadorian Andes. Tectonophysics 399, 351–380.

Boulangé, B., Vargas, C., Rodrigo, L.A., 1981. La sédimentation actuelle dans le lac Titicaca. Revue d'Hydrobiologie Tropicale 14, 299–309.

Cordani, U.G., Brito Neves, B.B., 1982. The geologic evolution of South America during the Archaean and Early Proterozoic. Revista Brasileira de Geociencias 12, 78–88.

Cordani, U.G., Sato, K., 1999. Crustal evolution of the South American Platform, based on Nd isotopic systematic on granitoid rocks. Episodes 22, 167–173.

Dosseto, A., Bourdon, B., Gaillardet, J., Allègre, C.J., Filizola, N., 2006. Time scale and conditions of weathering under tropical climate: study of the Amazon basin with U-series. Geochimica et Cosmochimica Acta 70, 71–89.

Dunne, T., Mertes, L.A.K., Meade, R.H., Richey, J.E., Forsberg, B.R., 1998. Exchanges of sediment transport between the floodplain and channel of the Amazon River in Brazil. Geological Society of America Bulletin 110, 450–467.

Espurt, N., Baby, P., Brusset, S., Roddaz, M., Hermoza, W., Regard, V., Antoine, P.O., Salas-Gismondi, R., Bolaños, R., in press. Influence of the Nazca Ridge subduction on the modern Amazonian retro-foreland basin. Geology.

Filizola, N., 1999. O Fluxo de Sedimentos em Suspensão nos Rios da Bacia Amazônica Brasileira. Dissertaçao de Mestrado, Universidade de Brasília, 63 p.

Filizola, N., 2003. Transfert sédimentaire actuel par les fleuves amazoniens. Thèse de doctorat, Université P. Sabatier, Toulouse, 292 p.

Gibbs, R.J., 1967. The geochemistry of the Amazon River system: Part I. The factors that control the salinity and the composition and concentration of the Suspended Solids. Geological Society of America Bulletin 78, 1203–1232.

Guyot, J.L., 1993. Hydrogéochimie des fleuves de l'Amazonie bolivienne. ORSTOM, Paris. 261 pp.

Guyot, J.L., Corbin, D., Quintanilla, J., Calle, H., 1991. Hydrochimie des lacs dans la région de Trinidad (Amazonie bolivienne). Influence d'un fleuve andin: le Rio Mamoré. Revue d'Hydrobiologie Tropicale 24, 3–12.

Guyot, J.L., Filizola, N., Quintanilla, J., Cortez, J., 1996. Dissolved solids and suspended sediment yields in the Rio Madeira basin, from the Bolivian Andes to the Amazon. Proc. Erosion and Sediment Yield: Global and Regional Perspectives. IAHS Publ., vol. 236, pp. 55–63.

Guyot, J.L., Filizola, N., Laraque, A., 2005. Régime et bilan du flux sédimentaire de l'Amazone à Óbidos (Pará, Brésil), de 1995 à 2003. Proc. Sediment Budgets. IAHS Publ., vol. 291, pp. 347–356.

Hemming, S.R., Biscaye, P.E., Broecker, W.S., Hemming, N.G., Klas, M., Hajdas, I., 1998. Provenance change coupled with increased clay flux during deglacial times in the Equatorial Atlantic. Palaeogeography, Palaeoclimatology, Palaeoecology 142, 217–230.

Holtzapffel, T., 1985. Les minéraux argileux. Préparation. Analyse diffractométrique et détermination. Publ. Société Géologique du Nord, Villeneuve d'Ascq. 136 pp.

Hoorn, C., Guerrero, J., Sarmiento, G.A., Lorente, M.A., 1995. Andean tectonics as a cause for changing drainage patterns in Miocene northern South America. Geology 23, 237–240.

Irion, G., 1983. Clay mineralogy of the suspended load of the Amazon and of rivers in the Papua–New Guinea mainland. Mitteilungen Geologie und Paläontologie Institut Universität Hamburg 55, 483–504.

Irion, G., 1984a. Clay minerals of Amazonian Soils. In: Sioli, H. (Ed.), The Amazon. W. Junk, Dordrecht, pp. 537–579.

Irion, G., 1984b. Sedimentation and sediments of Amazonian rivers and evolution of the Amazonian landscape since Pliocene times. In: Sioli, H. (Ed.), The Amazon. W. Junk, Dordretch, pp. 201–214.

Irion, G., 1991. Minerals in rivers. In: Degens, E.T., Kempe, S., Richey, J.E. (Eds.), Proc. Biogeochemistry of Major World Rivers. Scope, vol. 42. J. Willey, Chichester, pp. 265–281.

Johnsson, M.J., Meade, R.H., 1990. Chemical weathering of fluvial sediments during alluvial storage: the Macuapanim island point bar, Solimões River, Brazil. Journal of Sedimentary Petrology 60, 827–842.

Laraque, A., Céron, C., Armijos, E., Pombosa, R., Magat, P., Guyot, J.L., 2004. Sediments yields and erosion rates in the Napo River Basin: an Ecuadorian Andean Amazon tributary. Proc. Sediment Transfer through the Fluvial System. IAHS Publ., vol. 288, pp. 220–225.

Laraque, A., Filizola, N., Guyot, J.L., 2005. Variations spatio-temporelles du bilan sédimentaire dans le bassin amazonien brésilien, à partir d'un échantillonnage décadaire. Proc. Sediment Budgets. IAHS Publ., vol. 291, pp. 250–258.

Martinelli, L., Victoria, R.L., Dematte, J.L.I., Richey, J.E., Devol, A.H., 1993. Chemical and mineralogical composition of Amazon River floodplain sediments, Brazil. Applied Geochemistry 8, 391–402.

Masek, J.G., Isacks, B.L., Gubbels, T.L., Fielding, E.J., 1994. Erosion and tectonics at the margins of continental plateaus. Journal of Geochemical Exploration 99, 13941–13956.

Meade, R.H., Dunne, T., Richey, J.E., Santos, U.M., Salati, E., 1985. Storage and remobilization of suspended sediment in the lower Amazon River of Brazil. Science 228, 488–490.

Mégard, F., 1984. The Andean orogenic period and marginal and its major structure in central and northern Peru. Journal of the Geological Society (London) 141, 893–900.

Millot, G., 1964. Géologie des Argiles. Masson et Cie, Ed. Paris, 499 p.

Molinier, M., Guyot, J.L., Oliveira, E., Guimarães, V., 1996. Les Régimes Hydrologiques de l'Amazone et de ses affluents. In: Chevallier, P., Pouyaud, B. (Eds.), Proc. L'hydrologie Tropicale: Géoscience et outil pour le Développement. AIHS Publ., vol. 238, pp. 209–222.

Petschick, R., Kuhn, G., Gingele, F., 1996. Clay mineral distribution in surface sediments of the South Atlantic: sources, transport and relation to oceanography. Marine Geology 130, 203–229.

Räsänen, M., Neller, R., Salo, J., Jungner, H., 1992. Recent and ancient fluvial deposition systems in the Amazonian foreland basin, Peru. Geological Magazine 129, 293–306.

Roddaz, M., Viers, J., Brusset, S., Baby, P., Hérail, G., 2005. Sediment provenances and drainage evolution of the Neogene Amazonian foreland basin. Earth and Planetary Science Letters 239, 57–78.

Roddaz, M., Viers, J., Brusset, S., Baby, P., Boucayrand, C., Hérail, G., 2006. Controls on weathering and provenance in the Amazonian foreland basin: insights from major and trace element geochemistry of Neogene Amazonian sediments. Chemical Geology 226, 31–65.

Saleemi, A.A., Zulfiqar, A., 2000. Mineral and chemical composition of Karak Mudstone, Kohat Plateau, Pakistan: implications for smectite-illitization and provenance. Sedimentary Geology 130, 229–247.

Sombroek, W.G., 1984. Soils of the Amazon region. In: Sioli, H. (Ed.), The Amazon. W. Junk, Dordrecht, pp. 521–535.

Stallard, R.F., Edmond, J.M., 1983. Geochemistry of the Amazon. 2. The influence of geology and weathering environment on the dissolved load. Journal of Geophysical Research 88 (C14), 9671–9688.

Stanley, J.D., Wingerath, J.G., 1996. Nile sediment dispersal altered by the Aswan High Dam: the kaolinite trace. Marine Geology 133, 1–9.

Thiry, M., 2000. Palaeoclimatic interpretation of clay minerals in marine deposits: an outlook from the continental origin. Earth-Science Reviews 49, 201–221.